

# COLOUR-BASED AND CRITERIA-BASED METHODS FOR IMAGE FUSION

Oguz Gungor, Jie Shan

Geomatics Engineering, School of Civil Engineering, Purdue University, 500 Stadium Mall Drive,  
West Lafayette, IN 47907, USA - {ogungor, jshan}@ecn.purdue.edu

Commission VII, WG VII/6

## ABSTRACT:

Panchromatic and multispectral images are useful for the acquisition of geospatial information about the Earth surface for the assessment of land resources and environment monitoring. Panchromatic images usually have a better spatial resolution than the multispectral ones of the same sensor, while the multispectral images provide spectral properties of the objects. Image fusion methods are needed to find the missing spatial details in the multispectral images using the panchromatic ones and transfer these details into the multispectral images without or with limited spectral content distortion. This study addresses two classes of image fusion approaches: colour-based methods and statistical methods. Specifically, the traditional RGB to IHS transform is generalized from 3-D to n-D such that it can handle multiple image bands. As for the statistical methods, we propose a criteria-based approach that produces fusion products to meet a set of predefined desired properties. Principles, solutions, and formulation regarding these two approaches are presented. The proposed methods are tested with QuickBird images. Fusion results are evaluated visually and quantitatively with discussions on their properties.

## 1. INTRODUCTION

Remote sensing sensors capture the energy reflected or emitted from the objects and convert it into the digital numbers to form images. A sensor has a fixed signal to noise ratio associated to hardware design. An object can be detected only if sufficient amount of energy reaches the sensor. The energy to be collected by the sensor is related, among others, to IFOV (instantaneous field of view) of the sensor and the capability of the sensor to collect the energy over a certain spectral bandwidth.

IFOV of the sensor is inversely proportional to the spatial resolution of the image collected. The larger the IFOV, the lower the spatial resolution, since a sensor with a larger IFOV collects energy from a larger area on the ground. On the other hand, the amount of energy that reaches the sensor can also be increased by collecting the energy over a broader spectral bandwidth. This means that reducing the IFOV and increasing the capability of the sensor to collect energy over a larger spectral bandwidth may retain the spatial resolution of the image (Pradhan,2005). Panchromatic sensors collect the energy reflected by the objects over a broader spectral bandwidth with a narrower IFOV; therefore, panchromatic images have more spatial detail content than the multispectral images of the same sensor. This is why panchromatic images usually have a better spatial resolution than the multispectral images of the same sensor.

Image fusion intends to enhance the spatial details in the multispectral images by using the panchromatic ones. Over the last two decades various image fusion algorithms have been introduced (Pohl and van Genderen,1998). These methods are designed to accomplish two main tasks: extract the spatial details from the panchromatic image, and transfer them into the multispectral image using certain fusion rule or transform. Among the various types of image fusion methods, the study will address the colour-based methods and statistical methods.

The most representative colour-based approach is based on the RGB to IHS transform. The RGB colour space is ideal for

colour image generation. Images are displayed on monitors using RGB colour system and most image processing algorithms use RGB colour space for image processing applications. However, it has limitations (Gonzales and Woods,2003). The RGB colour space is not intuitive and not practical in colour selection. It is almost impossible to distinguish a colour from another only with RGB colour coordinates. In addition, it is device dependent. Different monitors and even an adjustment to the same monitor give different results. On the other hand, IHS colour space has a significant advantage over RGB colour space. IHS colour space makes possible to manipulate each colour attribute individually. In a multispectral image, spatial content is retained in the intensity component (Chibani and Houacine,2002) and spectral information is preserved in its hue and saturation components (Pohl and van Genderen,1998; González-Audicana et al.,2006). Using IHS colour space, the intensity component of an image can be changed without modifying its hue and saturation components. Due to this property of IHS colour space, it has been an ideal tool for image processing applications such as contrast enhancement and image fusion where the goal is enhancing the spatial content of the image while preserving its spectral properties.

Statistical image fusion methods transfer the spatial detail from the panchromatic image using the statistical properties of the input panchromatic and the multispectral images. These methods include principal component analysis (PCA), linear regression method (Price,1999), spatially adaptive image fusion (Park and Kang, 2004) and  $\sigma$ - $\mu$  methods (Gungor and Shan,2005, 2006), all of which have clear statistical interpretations.

In this study, we will present two approaches, respectively, in the categories of colour-based fusion methods, and statistical fusion methods. In the colour based approach, the classical RGB-IHS transform will be generalized from 3-D space to n-D space so that it can handle any number of bands of multispectral images. It is shown that the generalized IHS transform is

essentially a wavelet transform in the spectral domain of the input image as opposed to the spatial domain as most often discussed in the literatures. As for the statistical fusion approach, a criteria-based solution is proposed. This is an enhancement and modification to the published  $\sigma$ - $\mu$  approach (Gungor and Shan,2005, 2006). The new method starts from designing the desired properties for the fused images, and then uses them as criteria to solve a system of equations to determine the pixel values for the fused imagery. This way the resultant fusion outcome should have such desired properties and are optimal in terms of these predefined criteria. Through this approach, we develop a novel image fusion framework that is user and application driven such that the properties of the fused image are known beforehand. It can produce the fusion outcome with desired properties based on user's need, whereas the fusion outcome from other existing methods have unknown properties and must be evaluated in a case-by-case basis. The proposed image fusion techniques are tested by fusing QuickBird panchromatic image. Fusion results are evaluated along with discussions on the properties of the proposed fusion methods.

## 2. GENERALIZED RGB-IHS TRANSFORM

To generalize the IHS transform to support n multispectral bands, we first consider the traditional RGB to IHS transform, where there are only three bands involved. Harrison and Jupp,(1990) define an auxiliary Cartesian coordinate system  $I, V_1, V_2$  and the transform matrix  $T_3$  between these two spaces.

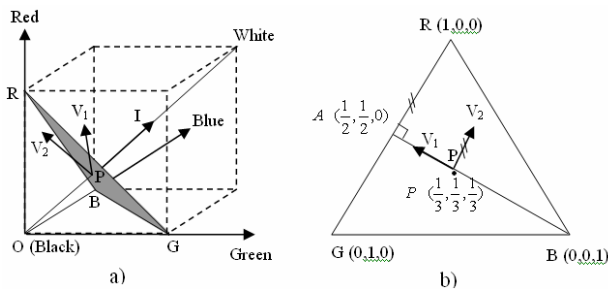


Figure 1. Relation between RGB and IHS Spaces

In the  $I, V_1, V_2$  system,  $I$  stands for the intensity and is defined as the line which connects the origin of the RGB colour space 'O' to the point 'White' (see Figure 1a). Using the coordinates of the vertices of  $\Delta RBG$  in Figure 1b, the coordinates of 'P' (the centre of  $\Delta RBG$ ) and 'A' (the middle point of line  $\overline{GR}$ ) can be determined as  $P(\frac{1}{3}, \frac{1}{3}, \frac{1}{3})$  and  $A(\frac{1}{2}, \frac{1}{2}, 0)$ . The orthonormal vector defining the direction of  $I$  can then be written as  $y_1^3 = (\frac{1}{\sqrt{3}}, \frac{1}{\sqrt{3}}, \frac{1}{\sqrt{3}})$ . Here, the subscript "1" indicates that  $I$  is the first vector and the superscript "3" denotes the dimensionality. The other two vectors  $V_1$  and  $V_2$  are defined on the  $\Delta RBG$  plane.  $V_1$  is defined in the direction

of  $\overline{BA}$  as perpendicular to the  $I$  axis, and  $V_2$  is chosen as perpendicular to  $V_1$ . The orthonormal vectors for  $V_1$  and  $V_2$  are obtained as  $y_2^3 = (\frac{1}{\sqrt{6}}, \frac{1}{\sqrt{6}}, \frac{-2}{\sqrt{6}})$  and  $y_3^3 = (\frac{1}{\sqrt{2}}, \frac{-1}{\sqrt{2}}, 0)$ . Thus the forward RGB to IHS transform is described as follows (Harrison and Jupp,1990)

$$\begin{bmatrix} I \\ V_1 \\ V_2 \end{bmatrix} = \begin{bmatrix} \frac{1}{\sqrt{3}} & \frac{1}{\sqrt{3}} & \frac{1}{\sqrt{3}} \\ \frac{1}{\sqrt{6}} & \frac{1}{\sqrt{6}} & \frac{-2}{\sqrt{6}} \\ \frac{1}{\sqrt{2}} & \frac{-1}{\sqrt{2}} & 0 \end{bmatrix} \begin{bmatrix} R \\ G \\ B \end{bmatrix} \quad (1)$$

To generalize the above relationship from 3-D to n-D, we first examine the 2-D case. The normalized intensity vector for 2-D would be  $y_1^2 = (\frac{1}{\sqrt{2}}, \frac{1}{\sqrt{2}})$ . The other normalized vector orthogonal to  $y_1^2$  is  $y_2^2 = (\frac{1}{\sqrt{2}}, \frac{-1}{\sqrt{2}})$ . Thus, the 2-D transform matrix is

$$T_2 = \begin{bmatrix} \frac{1}{\sqrt{2}} & \frac{1}{\sqrt{2}} \\ \frac{1}{\sqrt{2}} & \frac{-1}{\sqrt{2}} \end{bmatrix} \quad (2)$$

For 3-D, the intensity axis is  $y_1^3 = (\frac{1}{\sqrt{3}}, \frac{1}{\sqrt{3}}, \frac{1}{\sqrt{3}})$ . The third vector  $y_3^3 = (\frac{1}{\sqrt{2}}, \frac{-1}{\sqrt{2}}, 0)$  can also be obtained directly from the 3-D transform matrix  $T_2$  by simply adding a zero to  $y_2^2$  as the last element. Finally, the second vector  $y_2^3$  can be calculated as  $y_2^3 = (\frac{1}{\sqrt{6}}, \frac{1}{\sqrt{6}}, \frac{-2}{\sqrt{6}})$  which is orthonormal to  $y_1^3$  and  $y_3^3$ . Thus the transform  $T_3$  is (as given in Eq. 1)

$$T_3 = \begin{bmatrix} \frac{1}{\sqrt{3}} & \frac{1}{\sqrt{3}} & \frac{1}{\sqrt{3}} \\ \frac{1}{\sqrt{6}} & \frac{1}{\sqrt{6}} & \frac{-2}{\sqrt{6}} \\ \frac{1}{\sqrt{2}} & \frac{-1}{\sqrt{2}} & 0 \end{bmatrix} \quad (3)$$

Using the intensity definition given for 3-D above, the first axis in 4-D would be  $y_1^4 = (\frac{1}{\sqrt{4}}, \frac{1}{\sqrt{4}}, \frac{1}{\sqrt{4}}, \frac{1}{\sqrt{4}})$ . The two orthogonal vectors  $y_3^4$  and  $y_4^4$  can directly be copied from  $y_2^3$  and  $y_3^3$  by adding zeroes as the last elements as  $y_3^4 = (\frac{1}{\sqrt{6}}, \frac{1}{\sqrt{6}}, \frac{-2}{\sqrt{6}}, 0)$ ,  $y_4^4 = (\frac{1}{\sqrt{2}}, \frac{-1}{\sqrt{2}}, 0, 0)$ . Finally, we form  $y_2^4 = (\frac{1}{\sqrt{12}}, \frac{1}{\sqrt{12}}, \frac{1}{\sqrt{12}}, \frac{-3}{\sqrt{12}})$  to be orthonormal to  $y_1^4, y_3^4, y_4^4$ . The transform  $T_4$  in 4-D is

$$T_4 = \begin{bmatrix} \frac{1}{\sqrt{4}} & \frac{1}{\sqrt{4}} & \frac{1}{\sqrt{4}} & \frac{1}{\sqrt{4}} \\ \frac{1}{\sqrt{12}} & \frac{1}{\sqrt{12}} & \frac{1}{\sqrt{12}} & \frac{-3}{\sqrt{12}} \\ \frac{1}{\sqrt{6}} & \frac{1}{\sqrt{6}} & \frac{-2}{\sqrt{6}} & 0 \\ \frac{1}{\sqrt{2}} & \frac{-1}{\sqrt{2}} & 0 & 0 \end{bmatrix} \quad (4)$$

In general, the n-D transform matrix can be written as  $T_n$

$$T_n = \begin{bmatrix} \frac{1}{\sqrt{n}} \\ \frac{1}{\sqrt{(n-1)n}} \\ \vdots \\ \frac{1}{\sqrt{(n-i+1)(n-i+2)}} \end{bmatrix} \quad (5)$$

A number of evaluations can be made on the above generalized IHS (GIHS) transform. First, a variation of the above transform may be derived based on a different calculation of the intensities. As shown in the equations, we have used the normalized vector as the intensity calculation. In fact, the average of the involved bands may also be used as intensity (Zhou et al.,1998; Nunez et al. 1999;Wang et al.,2005; Choi,2006; González-Audicana et al.,2006), which would lead to different yet similar transform. Moreover, the order of the rows in the transform is not significant and the rows are interchangeable, however, it is recommended to keep the intensity as the first row. Finally, the generalized transform can be interpreted in terms of a wavelet transform in the spectral domain across different bands at one pixel location. It can be seen from Eq. 4 that the first row of the transformed image is the average of all the input bands (i.e., the intensity, up to a constant); this corresponds to the average spectral response at this pixel location and can be interpreted as the low frequency component in a wavelet transform. The second row is the difference between the average of the first three bands and the fourth band, which corresponds to a high frequency component among the bands. Similarly, the third row is the difference between the average of the first two bands and the third band, while the last row is the difference of the first two bands, all up to a normalization factor. Therefore, it is found that the generalized IHS (so is the classical IHS) transform is essentially equivalent to a wavelet transform in the spectral domain, where the first component is the intensity or band average, and the other components are band differences relative to band averages calculated in a sequential combination of the involved bands, all up to a constant.

To apply the above transform to image fusion, the input multispectral bands will first be transformed to a transformed space (equivalent to IHS in 3-D) with Eq. 3, 4 or 5. The transformed intensities are then replaced by the gray values in

the panchromatic image. As the last step, the fused image bands are obtained with a reverse transform  $T_n^{-1}$ .

### 3. CRITERIA-BASED IMAGE FUSION

The criteria-based image fusion method modifies the  $\sigma$ - $\mu$  method introduced by (Gungor and Shan,2005, 2006). The underlying principle is that the fused image should meet certain desired properties represented by a set of predefined criteria. The method forms the fused images as a linear combination of the input panchromatic and the upsampled multispectral images

$$F_k(m, n) = a_k(m, n) \cdot I_0(m, n) + b_k(m, n) \cdot I_k(m, n) \quad (6)$$

where  $m$  and  $n$  are the row and column numbers,  $k = 1, 2, \dots, N$  ( $N =$  number of multispectral bands),  $F_k$  is the fused image,  $I_0$  is the input panchromatic image,  $I_k$  is the  $k$ -th band of the resampled multispectral image, and  $a$  and  $b$  are the weighting factors for pixel location  $(m, n)$ , which control the amount of contribution from the panchromatic image and multispectral bands, respectively. The fusion formulation needs to determine the  $a$  and  $b$  coefficients at every pixel location, for which rules or criteria must be set. The selected criteria will determine the properties of the fusion outcome. Considering that image fusion is to retain the high spatial information or details from the panchromatic image and the spectral information or color from the multispectral one, we introduce the following three criteria.

**Criterion 1:** The variance of the fused image should be equal to the variance of the corresponding panchromatic image, such that its spatial details, described by the variance, can be retained in the fused image. Based on Eq. 6 this statement can be expressed as

$$Cov(F_k, F_k) = a_k^2 \sigma_o^2 + 2a_k b_k \sigma_{ok} + b_k^2 \sigma_k^2 = \sigma_o^2 \quad (7)$$

**Criterion 2:** The mean of the fused image should be equal to the corresponding mean of the multispectral image such that the color content, described by the mean, is retained in the fused image. Based on Eq. 6 the above statement can be expressed as

$$mean(F_k) = a_k \mu_o + b_k \mu_k = \mu_k \quad (8)$$

In Eq.7 and Eq.8, the notations for image location  $(m, n)$  are omitted for a clearer expression.  $a_k$  and  $b_k$  coefficients are used to construct the fused pixel at  $(m, n)$ .  $\sigma_o^2$ ,  $\sigma_k^2$  and  $\sigma_{ok}$  are the

variances of the panchromatic image and the  $k$ -th band, and the covariance between them.  $mean(F_k)$  is the mean of the fused band,  $\mu_o$  and  $\mu_k$  are the means of the corresponding panchromatic image and the  $k$ -th band of the multispectral image.

Combination of Criterion-1 and Criterion-2 provides a fused image that has the same variance as the panchromatic image and the same mean as the multispectral one. Therefore, the fused image is forced to have the same spatial variation as the panchromatic image which enables the injection of the spatial detail content of the panchromatic image into the fused multispectral one. In addition, the fused image is forced to have the same color content as the original multispectral image since the mean of the fused image is required to be the same as the mean of the multispectral one.

**Criterion 3:** This is to keep the inter-band relationships among the original multispectral bands after fusion. This criterion is inherited from the Brovey type fusion method

$$F_k(m, n) = C(m, n) \cdot I_k(m, n) \quad (9)$$

where  $C$  is a common coefficient for all  $N$  bands at pixel  $(m, n)$ , which assures that the ratio among the original multispectral bands are kept in the fused bands. It should be noted that the  $C$  factor varies from pixel to pixel.

Combining all the above four equations (Eq.6-9) will lead to an equation system for each pixel. At each pixel, each equation is written  $N$  times (one equation for each panchromatic and multispectral band) where  $N$  is the total number of multispectral bands. Therefore, a total of  $4N$  equations are written. There are  $3N$  unknowns ( $F_k, a, b$  for each band) in Eq. 6-8 and one unknown  $C$  in Eq. 9, which is common for all  $N$  bands. Therefore, there are  $r = (4N - (3N + 1)) = N - 1$  redundant equations for each pixel, i.e., the redundancy is one less than the total number of multispectral bands.

The solution to the equation system is obtained using the least squares technique. For the initial values of  $F_k$ , the pixel values of the corresponding original multispectral bands are used. Initial value of  $C$  is taken as 1, and the initial values of  $a_k$  and  $b_k$  are taken as 0.5. The criteria-based method employs small local windows on both panchromatic and resampled multispectral bands to find  $a_k, b_k$  and  $C$ . Hence, the variance and the mean values are calculated for the local windows. Besides, a  $1 \times 1$  window at the original multispectral image is chosen as the computation unit. Let  $M$  be the ratio of the resolutions of the multispectral and the panchromatic images. The area on the panchromatic and the resampled multispectral image corresponding to the smallest window on the original multispectral image is represented with a window size of  $M \times M$ . Larger window will yield sharper fused image, however, colour distortion will occur as pointed out by (Gungor and Shan, 2005). If the pixel values within the local window on the panchromatic

image are very uniform or all the same on occasion, the variance of panchromatic image  $\sigma_o^2$  essentially becomes zero. No spatial detail transfer is to be expected in this case; therefore, pixel values of the multispectral bands are kept unchanged and used for the fused pixels.

#### 4. EVALUATION AND DISCUSSIONS

The proposed GIHS method and the criteria-based method are tested by using QuickBird panchromatic (0.6m resolution) and multispectral images (2.4 m resolution). The imagery is over urban area in Purdue University campus in West Lafayette, Indiana. The fused multispectral images are shown in Figure 2 (GIHS method) and Figure 3 (criteria-based method).

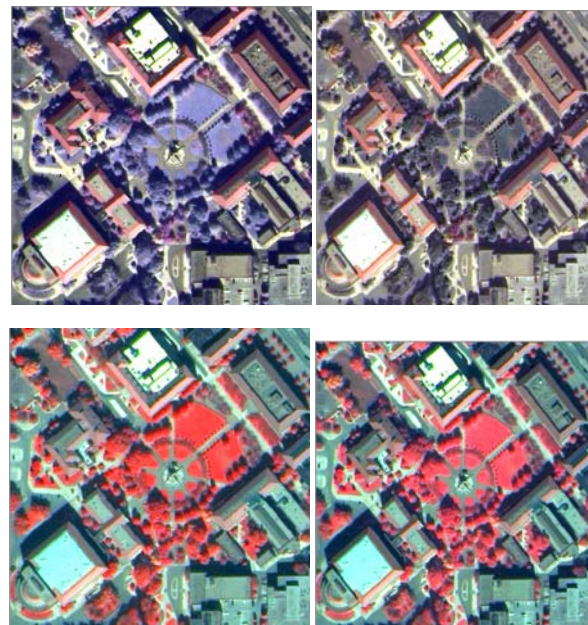


Figure 2. IHS (left) and GIHS (right) methods with B-G-R (top) and B-G-IR (bottom) display

It is evident from Figure 2 that the results of the classical IHS method, which are produced using blue, green and red bands, have significant colour distortion. The green colour of forest and grass becomes purple in these images. However, the results of the classical IHS method have good colour performance when blue, green and infrared bands are used. This is because the green colour of vegetation corresponds to high intensities (large gray values) in infrared band when compared to the other bands. This also affects the corresponding panchromatic image. The gray values of the panchromatic image become relatively larger than blue, green and red bands due to the effect of the infrared region. Therefore, discarding the infrared band in the intensity calculation causes more severe colour distortion than discarding the red band. On the other hand, the generalized IHS method uses all available bands to calculate the overall intensity. For this reason, the details to be added to each multispectral band are calculated by the contribution of all available bands. As seen from Figure 2 that the generalized IHS method gives better and more stable fusion results when the fused image is displayed using any three fused bands.

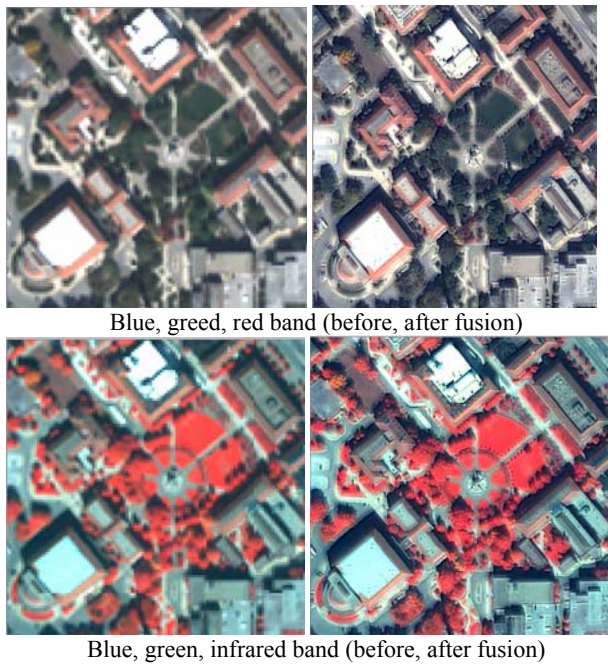


Figure 3. Input multispectral image (left) and fusion results (right) with the criteria-based approach

The criteria-based fusion method gives satisfactory fusion methods. Visual evaluation of Figure 3 shows that it produces appealing results when both spatial detail enhancement and the colour quality assurance are considered for the fused images. Because the fusion results are obtained based on pre-defined criteria its quality and properties are known. This can be treated as a general framework for image fusion, where users can design their own fusion tools based on pre-selected criteria.

The proposed methods are also evaluated quantitatively. A  $N$  band multispectral image is composed of spectral vectors whose elements consist of the gray values corresponding to the same pixel location on each band. SAM (Spectral Angular Mapper) denotes the absolute value of the angle between two spectral vectors in two image pairs. If the angle between these vectors is zero, then there is no spectral distortion between images. SAM is calculated in terms of degree or radians and averaged over the entire images to represent a global metric about spectral quality of the fused images (Alparone et al.,2007)

$$SAM = \arccos \left[ \frac{\langle v, \hat{v} \rangle}{\|v\|_2 \|\hat{v}\|_2} \right] \quad (10)$$

where  $v$  and  $\hat{v}$  are the spectral vectors in each pixel location in the multispectral and the fused images. Two spectral vectors in the original and the fused images may be parallel, but if their magnitudes are different, then radiometric distortion is introduced. The shortcoming of the SAM is that it is not capable of determining radiometric distortion in the fused images.

Wald,(2002) proposed a metric called ERGAS (“Erreur Relative Globale Adimensionnelle de Synthèse” in french)

which means “relative dimensionless global error in synthesis”. ERGAS index is given by (Alparone et al.,2007)

$$ERGAS = 100 \frac{h}{l} \sqrt{\frac{1}{N} \sum_{k=1}^N \left( \frac{RMSE(k)}{\mu(k)} \right)^2} \quad (11)$$

where  $h$  and  $l$  are the spatial resolutions of the panchromatic and the multispectral images, respectively. As an example, for QuickBird panchromatic and multispectral images,  $h/l$  is 1/4.  $N$  is the total number of the multispectral bands and  $\mu(k)$  is the mean of the  $k$ -th multispectral band.  $RMSE(k)$  is calculated between the  $k$ -th original and fused bands. Thus, ERGAS could consider the difference in the mean values of the fused and reference images, and catches any possible radiometric distortion.

Alparone et al.,(2004) proposed an index called Q4 to assess the quality of four band multispectral images by generalizing the Q index initially proposed by (Wang and Bovik,2002) for monochromatic images. Q4 is obtained by calculating the correlation coefficient between quaternions as

$$Q4 = \frac{|\sigma_{z_1 z_2}|}{\sigma_{z_1} \cdot \sigma_{z_2}} \cdot \frac{2 \cdot \sigma_{z_1} \cdot \sigma_{z_2}}{(\sigma_{z_1})^2 + (\sigma_{z_2})^2} \cdot \frac{2 \cdot |\bar{z}_1| \cdot |\bar{z}_2|}{|\bar{z}_1|^2 + |\bar{z}_2|^2} \quad (12)$$

The gray values of each spectral vector in the four-band reference and fused images constitute the real part of each quaternion  $z_1$  and  $z_2$ , respectively.  $|\sigma_{z_1 z_2}|$  is the modulus of the covariance between  $z_1$  and  $z_2$ ,  $\sigma_{z_1}$  and  $\sigma_{z_2}$  are the variances of  $z_1$  and  $z_2$ , and  $|\bar{z}_1|$  and  $|\bar{z}_2|$  are the modulus of the expectations of  $z_1$  and  $z_2$ . In Eq. 12, the first component is the hypercomplex correlation coefficient between the two spectral pixel vectors. The second and third components measure the contrast changes and mean bias on all bands simultaneously (Alparone et al.,2004). For this reason, Q4 is the most complete index to evaluate the fusion results in terms of both spatial and spectral quality. The range of the Q4 index is [0, 1], where 1 denotes that two images are identical.

In the quantitative evaluation, ERGAS and Q4 needs a reference multispectral image at the resolution of the fused images. However, there is no reference multispectral image at high spatial resolution prior to fusion. To solve this problem, (Laporterie-Déjean et al.,2005) obtain the reference images by simulating the sensor with high resolution data from an airborne platform (Alparone et al.,2007). On the other hand, (Wald,2002) degrade down the original panchromatic and multispectral images to a lower resolution in order to compare the fused product to the original multispectral image (Alparone et

al.,2007). This way, the original multispectral image can then be used as a reference for evaluation.

Methods	Quality measures		
	SAM	ERGAS	Q4
GIHS	2.26	6.15	0.53
Criteria-based	0.98	5.84	0.57

Table 1. SAM, ERGAS and Q4 values of the test methods

Table 1 lists the values of the three quality measures for the GIHS transform and criteria-based image fusion methods. The criteria-based image fusion method has a constraint (Eq. 9) to keep the ratio of the multispectral bands after fusion. Therefore, it has good SAM scores that are smaller than 1°. On the other hand, the SAM value in Table 1 suggests that the GIHS method would cause certain angular (2.3°) or colour distortion, which is consistent with visual evaluation on Figure 2.

As seen from Figure 2 and Figure 3, the fusion results from the GIHS transform and the criteria-based method are mostly comparable. This is shown by the very similar quality measure values in ERGAS and Q4, where the criteria-based approach shows slightly superior properties. When both spectral and spatial qualities of the fused images are considered, the criteria-based approach provides the adjustability to balance between these two considerations. These results imply that the criteria-based method can be an alternative to the popular colour-based methods since it has good spectral and spatial performance. Finally, it should be pointed out that both the GIHS transform method and the criteria-based approach can accommodate the fusion of multiple (>3) number of bands.

## 5. CONCLUSIONS

Two image fusion approaches have been developed and implemented. It is shown the classical IHS transform can be generalized to multiple dimensions such that image fusion can be performed with any number of bands under the concept of IHS transform. Furthermore, the generalized IHS transform is interpreted in terms of wavelet transform. It is shown that this transform is equivalent to a wavelet transform in spectral domain, where the first component is the intensity or band average, and the other components are band differences relative to band averages calculated in a sequential combination of the involved bands, all up to a constant. Tests demonstrate that the generalized IHS transform can produce stable and superior fusion results than the classical IHS transform approach.

The criteria-based image fusion method forms the fused images as the linear combination of the input panchromatic and multispectral images. Three criteria are introduced to determine the weighting coefficients which determine the contributions of the panchromatic and the multispectral images to construct the fused pixels. In the criteria-based fusion method, quality and properties of the fusion results are known since the results are obtained based on pre-defined criteria. This can be treated as a novel framework for image fusion, where users can design their own fusion tools based on their needs. In addition, the linear combination model provides the flexibility to balance the spatial quality and spectral quality in the final fusion outcome such that an optimal fusion result can be achieved. Tests results

along with visual and quantitative evaluations demonstrated that satisfactory fusion results can be obtained with the criteria-based method, whose performance is comparable and in general superior to colour-based ones, including the GIHS.

## REFERENCES

- Alparone, L., Baronti, S., Garzelli, A., and Nencini, F.,(2004). A Global Quality Measurement of Pan-Sharpned Multispectral Imagery. *IEEE Geoscience and Remote Sensing Letters*, Vol. 1, No. 4, pp. 313-317.
- Alparone, L., Wald, L., Chanussot, J., Thomas, C., Gamba, P., and Bruce, L. M.,(2007). Comparison of Pansharpening Algorithms: Outcome of the 2006 GRS-S Data-Fusion Contest. *IEEE Transactions on Geoscience and Remote Sensing*, Vol. 45, No. 10, pp. 3012-3021.
- Chibani, Y., and Houacine, A.,(2002). The Joint Use of IHS Transform and Redundant Wavelet Decomposition for Fusing Multispectral and Panchromatic Images. *International Journal of Remote Sensing*, Vol. 23, No. 18, pp. 3821-3833.
- Choi, M.,(2006). A New Intensity-Hue-Saturation Fusion Approach to Image Fusion with a Tradeoff Parameter *IEEE Transactions On Geoscience And Remote Sensing*, Vol. 44, No. 6, pp. 1672-1682
- González-Audicana, M., Otazu, X., Fors, O., and Alvarez-Mozos, J. (2006). A Low Computational-Cost Method to Fuse IKONOS Images Using the Spectral Response Function of its Sensors. *IEEE Transactions on Geoscience And Remote Sensing*, Vol. 44, No. 6, pp. 1683-1691.
- Gonzales, R. C., and Woods, R. E. (2003). *Digital Image Processing*. 2nd Edition. Pearson Education (Singapore) Pte. Ltd., Indian Branch, Delhi, India. ISBN: 8178086298
- Gungor, O., and Shan, J.,(2005). A Statistical Approach for Multi-resolution Image Fusion, UPPECORA 16UP - "Global Priorities in Land Remote Sensing", Sioux Falls Convention Center, Sioux Falls, SD, October 23-27.
- Gungor, O., and Shan J.,(2006). An Optimal Fusion Approach for Optical and SAR Images. *ISPRS Mid-term Symposium, Commission VII, "Remote Sensing: From Pixels to Processes"*, Enschede, the Netherlands, May 8-11.
- Harrison, B.A., and Jupp, D.L.B.,(1990). *Introduction to Image Processing*. CSIRO Publications. Canberra, Australia. ISBN 10: 0643050922.
- Laporterie-Déjean, F., de Boissezon, H., Flouzat, G., and Lefèvre-Fonollosa, M. J.,(2005). Thematic and Statistical Evaluations of Five Panchromatic/ Multispectral Fusion Methods on simulated PLEIADES-HR Images. *Information Fusion*, Vol. 6, No. 3, pp. 193-212.
- Núñez, J., Otazu, X., Fors, O., Prades, A., Palà, V., and Arbiol, R.,(1999). Multiresolution-Based Image Fusion with Additive Wavelet Decomposition. *IEEE Transactions on Geoscience and Remote Sensing*, Vol. 37, No. 3, pp. 1204-1211.
- Park, J. H., and Kang, M. G.,(2004). Spatially Adaptive Multi-resolution Multispectral Image Fusion. *International Journal of Remote Sensing*, Vol. 25, No. 23, pp. 5491-5508

Pohl, C., and van Genderen, J. L.,(1998). Multisensor image fusion in remote sensing: concepts, methods and applications. *International Journal of Remote Sensing*, Vol.19, No.5, pp. 823-854.

Pradhan, P.,(2005). Multiresolution Based, Multisensor, Multispectral Image Fusion. Ph.D. Dissertation. Mississippi State University. August 2005.

Price, J. C.,(1999). Combining Multispectral Data of Differing Spatial Resolution, *IEEE Transactions on Geoscience and Remote Sensing*, Vol. 37, No. 3, May, pp. 1199-1203.

Wald, L.,(2002). Fusion of Images of Different Spatial Resolutions. Presses de l'Ecole, Ecole des Mines de Paris, Paris, France, ISBN 2-911762-38-X, 200 pp

Wang, Z., and Bovik, A. C.,(2002). Universal Image Quality Index. *IEEE Signal Processing Letters*, Vol. 9, No. 3, pp. 81-84.

Wang, Z., Ziou, D., Armenakis, C., Li, D., and Li, Q.,(2005). A Comparative Analysis of Image Fusion Methods. *IEEE Transactions on Geoscience And Remote Sensing*, Vol. 43, No. 6, pp. 1391-1402.

Zhou J., Civco, D. L., and Silander J. A.,(1998). A Wavelet Transform Method to Merge Landsat TM and SPOT Panchromatic Data. *International Journal of Remote Sensing*. Vol. 19, No. 4, pp. 743-757.

